Procedia Manufacturing

Volume 1, 2015, Pages 840–853

43rd Proceedings of the North American Manufacturing Research Institution of SME http://www.sme.org/namrc

An Investigation of PDMS Stamp Assisted Mechanical Exfoliation of Large Area Graphene

Buddhika Jayasena* and Shreyes N. Melkote

[1]*The George W. Woodruff School of Mechanical Engineering*
Georgia Institute of Technology, Atlanta, Georgia, USA.
bjayasena3@me.gatech.edu, shreyes.melkote@me.gatech.edu

Abstract

We report on a study of a viscoelastic polymer stamp-based mechanical exfoliation technique capable of yielding large area (~square centimeters or larger) graphene layers from a highly ordered pyrolytic graphite (HOPG) substrate by manipulating the adhesion properties of a Polydimethylsiloxane (PDMS) stamp and other key process parameters. In particular, the effects of stamp adhesion, normal contact force, and dwell time on the exfoliation force, layer thickness, and graphene surface morphology are studied. Experiments show that the process is capable of exfoliating relatively large (up to 12x 12 mm^2) graphene layers under certain conditions. The exfoliated layers, albeit of varying thickness, have regions that are tens of nanometer thick and contain various topographical features such as bubbles, wrinkles, and compressed regions. This work serves as the first step toward developing a scalable production method for large area graphene and other layered materials of interest.

Keywords: Mechanical exfoliation, Graphene, Polymer adhesion, PDMS

1 Introduction

Scalable production of large area, defect-free, layered materials such as graphene, which is a two-dimensional 0.3 nm thick single layer of carbon atoms, is a much sought-after goal today due to their attractive optical, thermal, mechanical, and electronic properties. Till recently it was debated if it is thermodynamically possible for such single layer materials to exist (Novoselov et al., 2005). The groundbreaking work of Novoselov et al, (Novoselov et al., 2004) who were able to separate a single layer of graphene from graphite through micromechanical cleavage showed that these mono-layers can indeed exist (Novoselov et al., 2004). Graphene displays remarkable properties that are useful in many applications such as transparent conductive coatings, energy-storage devices, drug delivery, composite material, tissue engineering, regenerative medicine, etc. (Geim and Novoselov, 2007,

* Corresponding Author

Peer-review under responsibility of the NAMRI Scientific Committee
doi:10.1016/j.promfg.2015.09.073

Novoselov et al., 2012, Nair et al., 2008, Jang and Zhamu, 2008, Chang et al., 2010, Ruoff, 2008, Berman et al., 2014, Alberts et al., 2009). Many of these applications require large area, continuous graphene sheets that are flat and possess high purity continuous structure with no mechanical and chemical imperfections. Therefore, cost-effective production of mono- and/or few-layer graphene with minimal defects is an urgent challenge requiring the attention of manufacturing researchers. The application of this remarkable material largely depends on the reliable and scalable production of high quality large area sheets of graphene while preserving its unique physical and mechanical properties (Stankovich et al., 2006). The properties of graphene are known to be strongly influenced by the synthesis method (Allen et al., 2009).

Current graphene synthesis methods can be broadly classified into the following three groups: epitaxial growth, unconventional methods, and exfoliation techniques (Jayasena, 2014). In the epitaxial growth method, graphene is grown on top of a substrate using chemical or physical vapor deposition (CVD or PVD). While these chemically assisted methods are capable of producing large area graphene layers, they tend to have lower charge carrier mobility, which is a key factor in electronic applications, compared to mechanically exfoliated graphene (Novoselov et al., 2012). In addition, in these methods, single and multi-layers often overlap (Novoselov et al., 2012, de Heer et al., 2007). Unconventional methods include techniques such as unzipping Carbon Nanotubes (CNTs), arc discharge, and detonation of chemicals. The unzipping of CNTs is an attractive technique in which CNT is exposed to oxygen plasma or microwaves (Janowska et al., 2009, Humberto et al., 2012). The arc discharge technique involves the use of high current between a graphite anode and cathode in a hydrogen and helium atmosphere (Wu et al., 2009). In the chemical detonation method, a mixture of natural graphite, nitric acid, and CH_3NO_2 is exploded in a vessel and graphene sheets are harvested from the resulting soot (Sun et al., 2008). All of these methods suffer from limitations such as poor yield, use of hazardous chemicals, and contamination of graphene with impurities and functional groups, and long processing times.

Exfoliation process routes consist of chemical, thermal, and mechanical methods. In chemical and thermal exfoliation methods, colloidal suspension and intercalation techniques are used to produce mono and few-layer graphene (Stankovich et al., 2006, Goler et al., 2011). These techniques too suffer from some of the limitations described earlier (Meihua et al., 2010). The adhesive-tape (or Scotch tape) based mechanical exfoliation process is reported to be the best process for producing high quality graphene sheets, but suffers from low yield and small size of sheets (~ ten to hundred microns square) (Novoselov et al., 2012). At present, micromechanical cleavage techniques are predominantly restricted to laboratory-scale research activities. Another mechanical exfoliation method that uses an atomic force microscope (AFM) tip to scratch Highly Ordered Pyrolytic Graphite (HOPG) mesas has been reported (Xuekun et al., 1999, Zhang et al., 2005). Apart from these, a wedge based mechanical exfoliation technique was investigated in an attempt to address the large-scale production problem (Jayasena and Subbiah, 2011, Jayasena et al., 2013, B. Jayasena, 2014).

The "transfer printing" technique uses elastomeric stamps to transfer patterned micro or nano features from a donor substrate to a recipient substrate (Meitl, 2007). This technique is often referred to as "soft lithography" (Xia and Whitesides, 1998, Whitesides et al., 2001, Huang et al., 2005) and is used in a wide variety of applications including fabrication and assembly of micro sensors, micro-electromechanical systems (MEMS), micro-analytical systems, and micro-optical systems (Hua et al., 2004). Polydimethylsiloxane (PMDS) is the most common material used for mold/stamp making and its unique properties such as low stiffness, chemical stability, and conformal contact make it very versatile. Several attempts to transfer chemically grown graphene using a sacrificial polymer layer between the graphene layer and a polymer substrate (typically PDMS) have been reported (Matthew et al., 2005, Carlson et al., 2012, Kymissis and Cox, 2013, Chun-Hu et al., 2012). Several transfer-printing techniques have been reported to demonstrate the transfer of graphene and other materials by controlling the adhesion strength between the PDMS stamp and the material to be transferred or the receiving substrate. These techniques include a kinetically controlled method that relies on control of

the lift-off and printing speed (Matthew et al., 2005), a relief surface assisted method that uses relief structures on the stamp surface (Kim et al., 2010), a shear assisted method to control the delamination crack via shear loading (Carlson et al., 2011), a laser driven method that controls the detachment mechanism via laser pulse-induced thermal expansion of the stamp (Chang and Bard, 1991), and a pneumatically driven method that controls stamp-substrate adhesion through pressurized micro channel features built into the stamp (Carlson et al., 2012). Small stamp sizes (100 x 100 μm^2) are used in all of these studies. Although these studies speculate on the use of such PDMS stamp-based "transfer printing" methods to separate few layers of graphene, the lack of detailed knowledge of the specific process conditions necessary to realize this goal is a significant hurdle to establish it as a reliable and truly scalable graphene manufacturing process. In particular, detailed knowledge of the effects of PDMS elasticity and process variables such as the normal contact force, contact dwell time, and exfoliation speed on the exfoliation force, layer thickness and quality of the exfoliated layers is lacking. Although a limited attempt to manipulate the adhesion property of the PDMS stamp to separate graphene layers has been reported (Kwanghyun et al., 2013), it uses very small (400 x 400 μm^2) pre-fabricated chemically grown CVD mesas.

It is clear from the review that while some very good work on polymer stamp-based transfer printing has been reported, there is limited understanding of the effects of various process parameters on the exfoliation characteristics, which is essential for reliable and repeatable mechanical exfoliation of minimally-defective large area mono- and few-layer graphene from bulk graphite. This paper presents the results of an experimental investigation of the effects of PDMS stamp elasticity (and adhesion) and other process conditions such as the normal contact force, dwell time, and exfoliation speed on the exfoliation force, graphene layer thickness, and surface morphology.

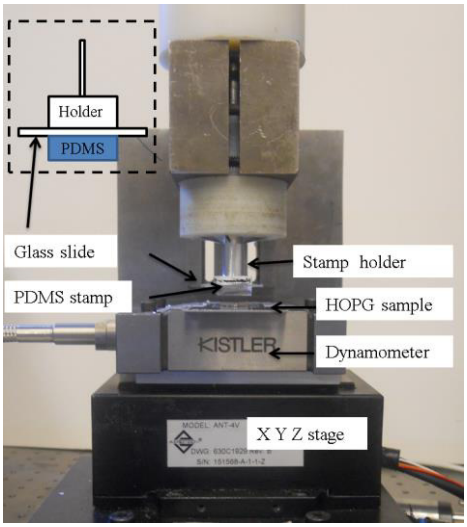

Figure 1: Experimental setup

2 Materials and Methods

2.1 Experimental Set-Up

A desktop-sized experimental setup (see Figure 1) was used to investigate the proposed exfoliation process. In its current form, the setup permits controlled study of the effects of normal contact force between the PDMS stamp and HOPG substrate, the dwell time prior to exfoliation, and

the exfoliation speed in the vertical direction. The instantaneous exfoliation forces in the X, Y, and Z directions were measured using a three-axis piezoelectric force dynamometer (Kistler 9256) mounted on stacked XYZ stages that have a few nanometer positioning resolution, a travel range of 25 mm in the X and Y directions, and 5 mm in the Z direction. Measured forces directed into the dynamometer surface are positive. An HOPG sample (12 x 12 x 2 mm^3, SPI-ZYA) was mounted on the dynamometer surface while the PDMS stamp was affixed to a glass slide that is attached to the stationary vertical section of the setup as shown in Figure 1. The stamp was fixed to the glass plate by natural adhesion of the PDMS. Preliminary testing showed that the chemical bond between the PDMS stamp and glass-slide is stronger than between the stamp and the HOPG sample. Therefore, no delamination occurred at the stamp-glass slide interface during the experiments.

2.2 Stamp Preparation

PDMS stamps were prepared using a Sylgard 184 monomer-curing agent kit. Specifically, mixing ratios (by weight) of 10:1 and 20:1 were used to vary the stamp elastic modulus and its corresponding adhesion properties. The two monomer-curing agent mixtures were stirred for 3 and 5 minutes, respectively, and degassed in a vacuum desiccator for 20 minutes under -0.8 KPa pressure. The mixtures were then poured into a 50 x 50 x 6.25 mm^3 glass container and cured for different time durations (20 to 80 minutes) in a furnace at 70^0 C. After completion of the cure cycle, the sample was removed from the furnace and placed in a freezer for 1 hour to arrest the rapid thermal softening normally observed after furnace curing. A 15 x 15 mm^2 PDMS stamp was cut from each cured sample and its elastic modulus and adhesiveness (measured qualitatively and quantitatively) were determined.

2.3 Stability of PDMS Stamp

The initial evaluation of stamp properties focused on two aspects: (i) understanding the variation in stamp elastic modulus (and therefore its conformability), and (ii) general adhesion characteristics (measured qualitatively by its stickiness ascertained by human touch) as a function of the furnace curing time and the post-furnace curing time. The effect of post-furnace curing time was evaluated to determine the mechanical stability of the stamp and its adhesion characteristics over an extended time period. The elastic modulus of each sample was measured using a tensile test at 5% strain in a Dynamic Mechanical Analyzer (DMA Q800). Figure 2a shows the variation in the stamp elastic modulus and its corresponding adhesiveness as a function of furnace curing time. In general, the adhesiveness of the stamps prepared using the 20:1 mixing ratio was found to be much greater than the 10:1 ratio, albeit its handleability was much worse. Stamp handleability improved with increase in its elastic modulus which increased with furnace curing time as seen in Figure 2a. It is also seen that there is an optimal furnace curing time for each mixing ratio in order to obtain sufficient stamp adhesion while permitting ease of handling. Based on this study, a 25 min furnace curing time was selected for the 10:1 mixing ratio and a 40 min curing time was selected for the 20:1 mixing ratio in order to achieve a good combination of stickiness (adhesion) and handleability. Figure 2b shows the post-curing ambient stability of the stamp elastic modulus for the two mixing ratios. This room temperature stability is important since any change in the adhesion characteristics during stamp use will impact the repeatability of the exfoliation process. Till now, these aspects are not explicitly discussed in the literature but are important from a standpoint of process scalability. It is seen from Figure 2b that after an initial decrease in the elastic modulus, there is a very stable operating region for both stamp compositions evaluated. The motivation for this investigation comes from the fact that the PDMS stamp elastic modulus, handleability, and its adhesion characteristics are closely linked and change with curing conditions. In order to tailor the adhesion property for exfoliating layered materials in a controlled manner, this understanding is crucial. The stickiness of the cured PDMS samples was also assessed quantitatively in terms of the adhesive strength as discussed next.

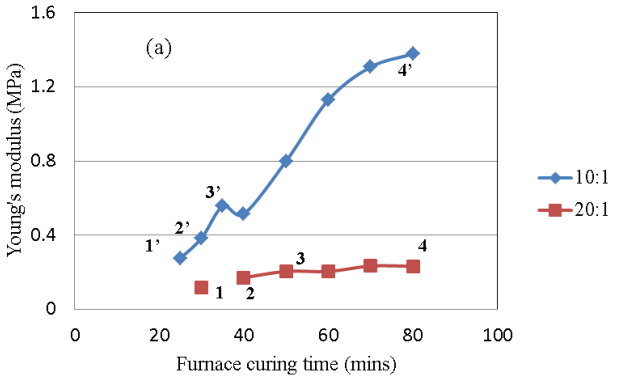

1. Very sticky, difficult to handle
2. Sticky, moderate handlability
3. Slightly sticky, moderate handleability
4. Less sticky, rigid

1'. Very sticky, difficult to handle
2' Sticky, handlability improved
3' Sticky and hard
4'. Not sticky, rigid

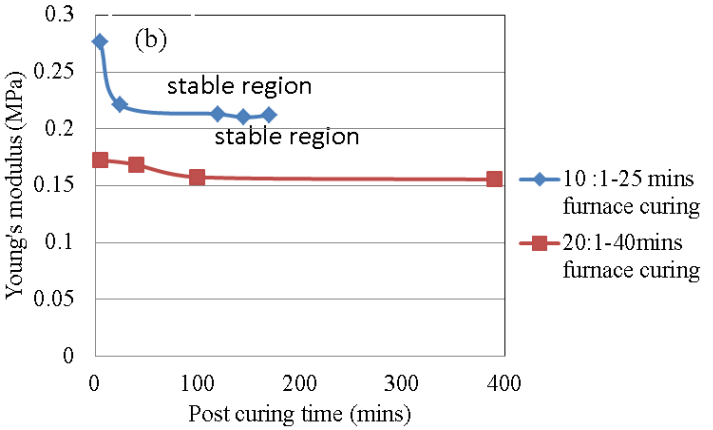

Figure 2: (a) Variation of the PDMS elastic modulus and corresponding adhesion characteristics with furnace curing time, (b) room temperature stability of the 10:1 and 20:1 mixing ratio cured PDMS samples.

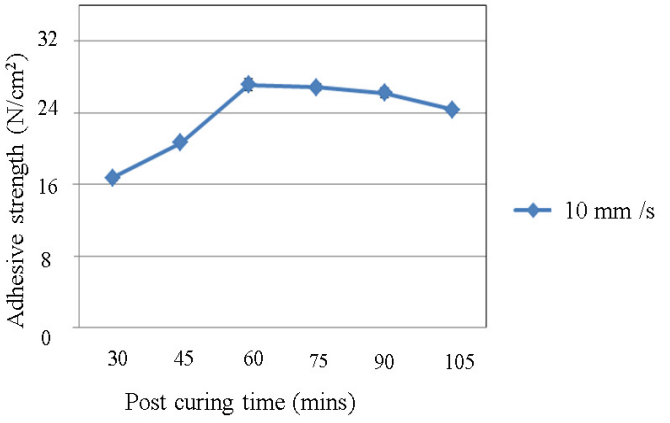

Figure 3: Stamp adhesion strength after post curing and freezing.

2.4 Adhesive strength of PDMS stamp

The adhesion strength of the PDMS stamps was quantified through a symbolic exfoliation process similar to the preliminary exfoliation work discussed earlier. Instead of using HOPG, a flat glass slide was rigidly fixed to the dynamometer surface. The normal contact force exerted by the stamp on the glass slide and the dwell time were kept constant at 15 N and 1 min, respectively, after which the stamp was withdrawn in the normal direction at 10 mm/s. The adhesion force per unit area during stamp withdrawal was measured and used as a quantitative measure of the adhesiveness of a given stamp composition and size. Figure 3 shows the variation of adhesive strength with post-curing time. While there is some variability in the adhesion strength over time, it remains fairly stable after approximately 60 mins. The repeatability of the adhesive strength at a given time was excellent (values varied by no more than 0.6 N/cm^2).

2.5 Exfoliation Experiments

A few exploratory tests were conducted on a mid-range quality HOPG substrate (SPI-ZYH) to ascertain the stamp performance and to understand the exfoliation force signature. In these tests, the normal contact force and the initial dwell time between the stamp and the HOPG substrate were kept constant at 15 N and 1 minute, respectively, and the exfoliation speed (in the vertical direction) was varied between 1 and 5 mm/s. Stamps made from the 10:1 mixing ratio were used in these tests. The tests showed that yield was maximum at 5 mm/s. Following the exploratory tests, a full-factorial experiment was executed using the higher quality HOPG substrate (SPI-ZYA), the same PDMS mixing ratio, and the factors and levels listed in Table 1. Each test condition was repeated three times. The exfoliation speed was constant at 5 mm/s. In these experiments, the effects of normal contact force and dwell time on the morphology and thickness of graphene layers and the exfoliation force were analyzed.

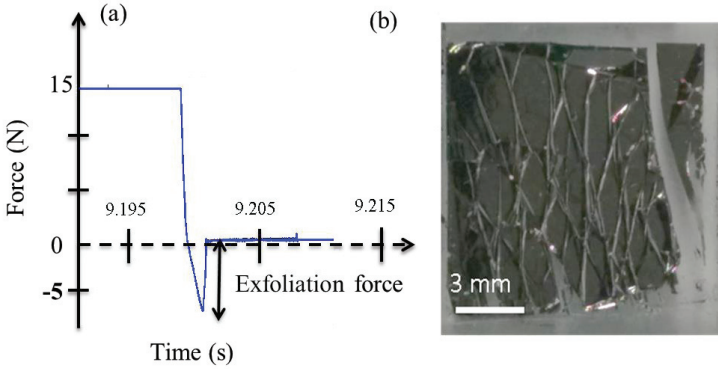

Figure 4: (a) Experimentally measured exfoliation force profile (Note: force is measured positive into the HOPG sample), (b) corresponding exfoliated surface morphology (Test 10) with ZYA grade

3 Results and Discussion

The preliminary tests with the 10:1 PDMS stamp and varying exfoliation speed indicated that, in general, the area of the exfoliated layer increases with exfoliation speed and the largest area (on the order of a few square millimeters) is obtained at a speed of 5 mm/s. A representative exfoliation force signature is shown in Figure 4. Note that the force is positive when directed into the HOPG sample. Hence, the exfoliation force is negative. As the stamp is retracted from the HOPG substrate, the force in the normal (Z) direction first decreases rapidly before increasing and leveling off after exfoliation is

complete. Note that the separation of graphite layers (adhered to PDMS stamp) from the HOPG substrate starts when the force signature starts to increase (bottom portion of the force profile in Figure 4a). The weak van der Waals bonds between the graphite layers allow decoupling of adjacent layers under an external stress. The strong adhesion forces between the surface of the PDMS stamp and the HOPG surface cause the weak secondary bonds between the graphite layers to be overcome. Figure 4b shows the morphology of a large exfoliated sheet. A number of wrinkles and folds in the sheet are clearly visible. Some of these defects are due to the average quality of the HOPG substrate used while the rest are attributed to the exfoliation process. These defects are discussed in more detail later in the paper.

Test No	Normal contact force (N)	Dwell time (mins)
1	5	1
2	5	5
3	5	10
4	5	1
5	5	5
6	5	10
7	5	1
8	5	5
9	5	10
10	10	1
11	10	5
12	10	10
13	10	1
14	10	5
15	10	10
16	10	1
17	10	5
18	10	10
19	15	1
20	15	5
21	15	10
22	15	1
23	15	5
24	15	10
25	15	1
26	15	5
27	15	10

Table 1: Process parameters and their levels

3.1 Surface Morphology of Exfoliated Layers

The surface morphologies of the exfoliated layers were characterized using confocal microscopy. In general, the dimensions of the exfoliated layers are significantly larger than those obtained in other exfoliation techniques reported in the literature (Novoselov et al., 2012). Specifically, under certain process conditions, exfoliated layers as large as 12 x 12 mm^2 were obtained (see Figure 4b). Due to the large sizes and a limited field of view of the confocal microscope, only selected portions of the measured surface morphologies are shown in Figure 5. A variety of surface features including large flat patches, compressed regions, wrinkles, torn edges, folds, and bubbles are observed in the layers

under different exfoliation conditions. Figure 5a highlights (circled) a crumpled region. Wrinkles, seen in Figure 5b and 5c, and step folds, seen in Figure 5f, are frequently observed on the surface as reported elsewhere in the literature (Zang et al., 2013). Straight, torn, and folded edges are seen in Figure 5e and Figure 5f (see circled regions). Figure 5d indicates bi-axially compressed (or crumpled) features that span a larger area, analogous to those reported in (Kymissis and Cox, 2013). It is crucial to understand how to control such defects or structures in order to exfoliate much cleaner few layers of graphene. The defects in the observed surface morphologies are attributed to several causes including uneven force distribution between the PDMS stamp and the HOPG, stretching of the graphite surface due to PDMS elasticity during initial contact followed by relaxation of the strains during exfoliation, and pre-existing defect structures in the as-received mid-quality HOPG material. Under certain conditions, fragmented and partially exfoliated layers were observed on the PDMS stamp surface.

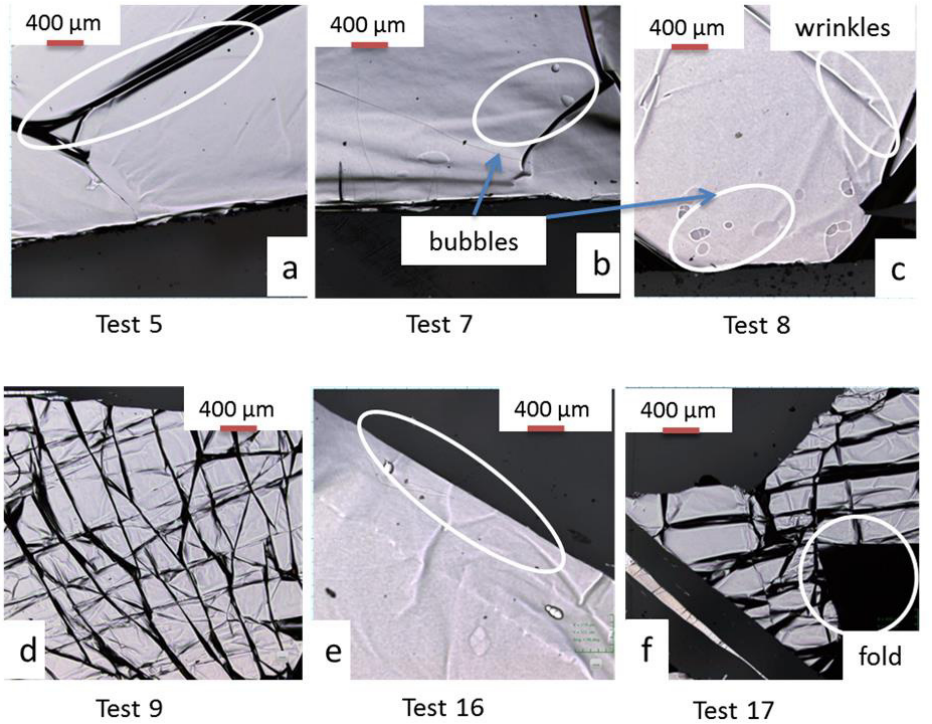

Figure 5 : Morphologies of exfoliated layers under various conditions. (a) crumpled region, (b) bubbles and torn edges, (c) wrinkles and bubbles, (d) large areas of uni and bi-axially compressed regions, (e) straight edges, and (e) layers with folds in them.

3.2 Thickness of Exfoliated Layers

The thickness of the exfoliated layers was measured using confocal microscopy. A defect free edge in a relatively flat portion of the exfoliated layer produced in each experiment was selected for thickness measurement. It should be noted that several experiments yielded layers with areas of sub-micrometer thickness. Figure 6a shows a sample section of exfoliated graphene layers and the corresponding thickness measurement locations. Some of the sub-micrometer thickness regions were further characterized using an Atomic Force Microscope (AFM). Note that the scanning area of the AFM is 40 x 40 μm^2, which is much less than the area measured in the confocal microscope. Figure 7 shows a representative AFM measurement of the edge of an exfoliated layer. It is seen that the thickness of the selected region in the AFM measurement is around 70 nm. Regions with thickness in

excess of 1 µm were also found indicating the need for further process optimization to achieve thinner (mono- or few-) layers of graphene.

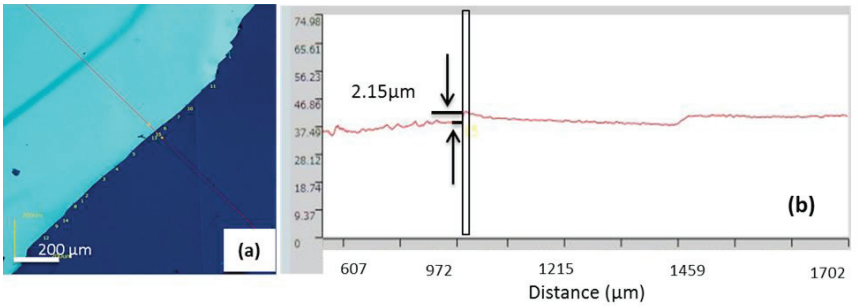

Figure 6: Selected confocal microscope measurement (Test 11); (a) 15 thickness measurements taken along the visible edge, (b) cross-sectional view.

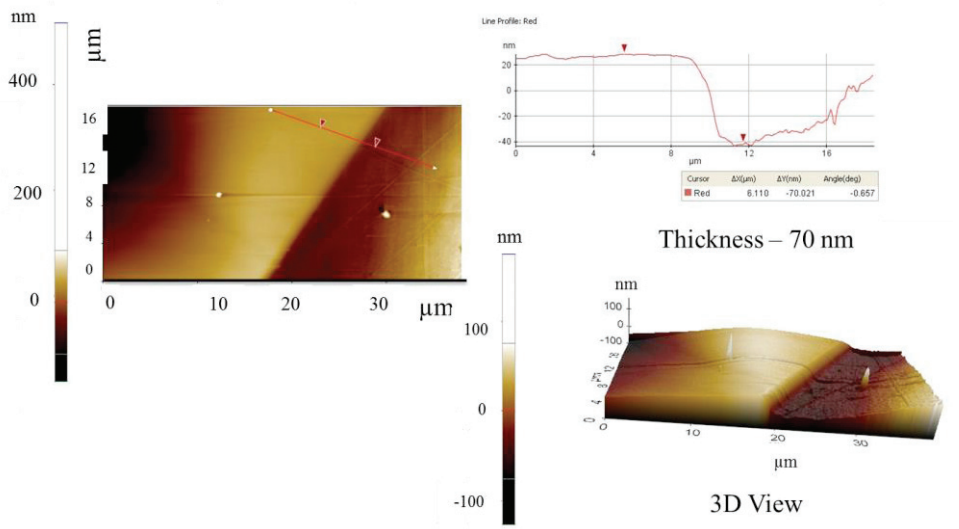

Figure 7: AFM measurement of layer thickness; cross-section and 3-D view (Test 11).

3.3 Correlation of Exfoliation Force and Layer Thickness

The measured exfoliation forces and the corresponding minimum layer average thicknesses are plotted in Figure 8. Figure 8a represents the exfoliation force trend corresponding to the 5 N normal contact force tests. It appears from this figure that the exfoliation force and the corresponding minimum layer thickness are roughly correlated since they tend to exhibit similar trends. The circled data points represent tests where the exfoliated surface area was almost equal to the entire contact area of the PDMS stamp. Figure 8b and 8c show the exfoliation force vs. average layer thickness trends for the 10N and 15N normal force cases, respectively. However, there does not appear to be a direct correlation between the exfoliation force and average layer thickness for these two cases. In general, the exfoliation force is between 3 and 6 N in almost all cases.

The main effect plots for the factorial experiment are shown in Figure 9. These plots suggest the existence of an optimum combination of normal contact force, and dwell time to obtain the thinnest layer of graphene. The mean effect of dwell time is consistent in that the increase in dwell time appears to increase the layer thickness.

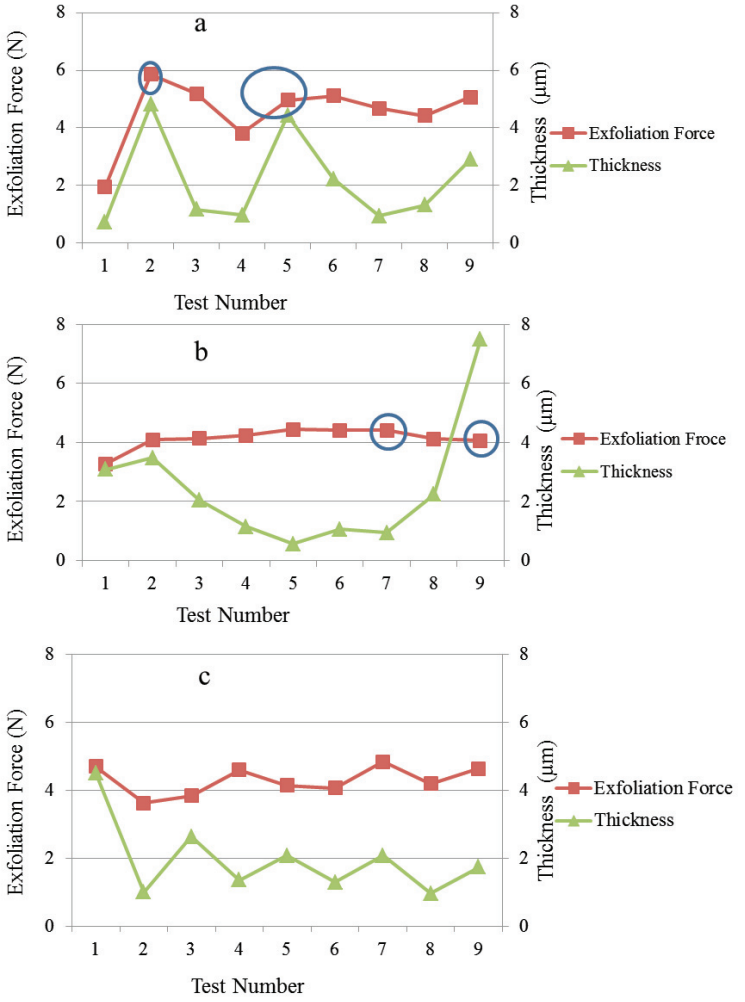

Figure 8: Comparison of exfoliation force and exfoliated layer thickness for different normal contact force values: - (a) 5 N, (b) 10 N, (c) 15 N. The circled test conditions yield the largest size (12 x 12 mm^2) graphene layers.

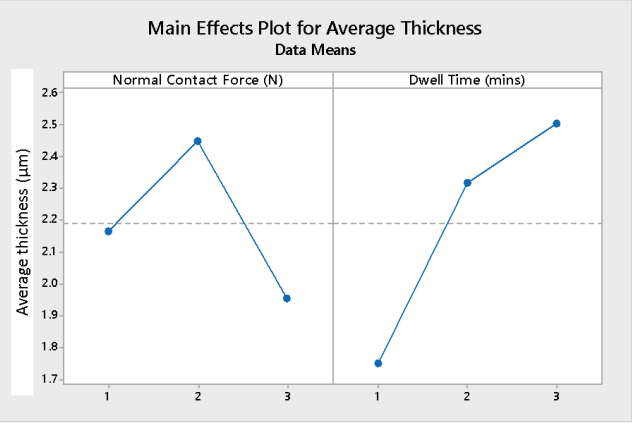

Figure 9 : Main effects plot

Based on the above results, a dwell time of 1 minute and speed of 5 mm/s were selected and the normal contact force varied to test the repeatability of the observed exfoliation force and layer thickness trends. Figure 10 shows a comparison of the exfoliation force obtained in the repetitions and those obtained earlier in the full-factorial experiment. It is seen that the exfoliation force is quite repeatable and tends to be in the range of 3.5-5.5 N, irrespective of the normal contact force magnitude. Similarly, AFM thickness measurements indicate that the layer thickness is also quite repeatable (see Figure 10). While these results are preliminary, they do show the ability of the PDMS stamp based mechanical exfoliation process to produce large area graphene layers, albeit of much higher thickness than eventually desired. Further process optimization is clearly required to achieve thinner exfoliated layers and will be pursued in future work.

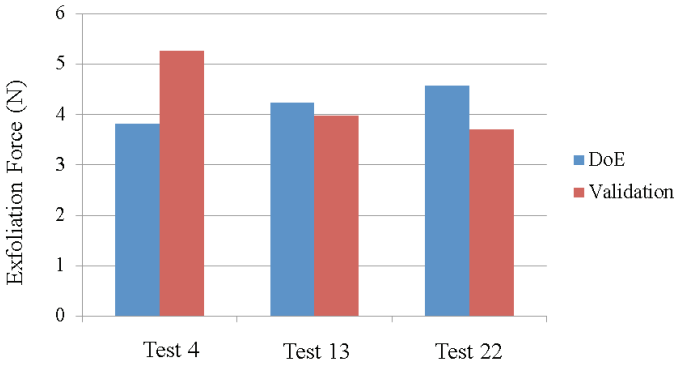

Figure 10: Repeatability of exfoliation force

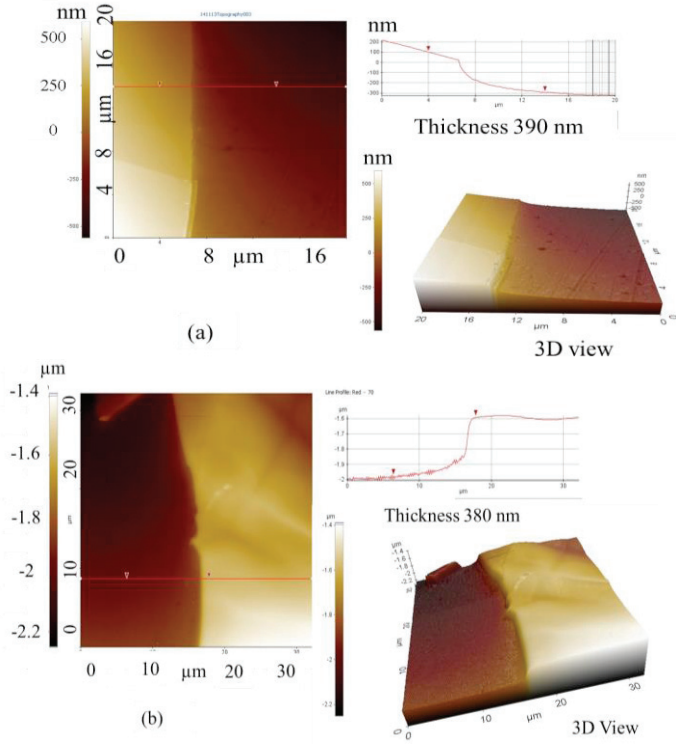

Figure 11: (a) Thickness measurement in DOE and (b) repeated experiment (Test 22)

4 Conclusions

The results of an investigation of a PDMS stamp assisted mechanical exfoliation process for producing large area graphene sheets from a HOPG substrate was presented in the paper. It was found that the process is capable of yielding large area (up to 12 x 12 mm^2) multi-layer graphene with thickness ranging from tens of nanometers to a few microns. A number of surface defects such as wrinkles, folds, compressed regions, and tears are observed in the exfoliated layers. The results also suggest a possible correlation between the exfoliation force and exfoliated layer thickness for a low normal contact force. Further investigations are underway to achieve exfoliation of few-layer large area graphene sheets of uniform thickness by fine-tuning the process conditions.

Acknowledgement

We acknowledge partial funding for this work from the Morris M. Bryan Jr. Professorship. We also thank Professor Zhigang Jiang and his students in the School of Physics at Georgia Tech for their help with the AFM measurements. Finally, we are grateful to the anonymous reviewers for their insightful comments, which contributed to improving our work and paper quality.

References

Alberts, M., Kalaitzidou, K. and Melkote, S. (2009), "An investigation of graphite nanoplatelets as lubricant in grinding", *International Journal of Machine Tools and Manufacture,* vol 49**,** pp. 966-970.

Allen, M.J., Tung, V.C. and Kaner, R.B. (2009), "Honeycomb carbon: A review of graphene", *Chemical Reviews,* vol 110**,** pp 132-145.

Berman, D., Erdemir, A. and Sumant, A.V. (2014), "Graphene: A new emerging lubricant", *Materials Today,* vol 17**,** pp. 31-42.

Carlson, A., Kim-Lee, H.J., Wu, J., Elvikis, P., Cheng, H., Kovalsky, A., Elgan, S., Yu, Q., Ferreira, P.M., Huang, Y., Turner, K.T. and Rogers, J.A. (2011), "Shear-enhanced adhesiveless transfer printing for use in deterministic materials assembly", *Applied Physics Letters,* vol 98, pp. 264104

Carlson, A., Wang, S., Elvikis, P., Ferreira, P.M., Huang, Y. and Rogers, J. A. (2012), "Active, programmable elastomeric surfaces with tunable adhesion for deterministic assembly by transfer printing", *Advanced Functional Materials,* vol 22**,** pp. 4476-4484.

Chang, H. and Bard, A.J. (1991), "Observation and characterization by scanning tunneling microscopy of structures generated by cleaving highly oriented pyrolytic graphite", *Langmuir,* vol 7**,** pp. 1143-1153.

Chang, H., Wang, G., Yang, A., Tao, X., Liu, X., Shen, Y. and Zheng, Z. (2010), "A transparent, flexible, low-temperature, and solution-processible graphene composite electrode", *Advanced Functional Materials,* vol 20**,** pp. 2893-2902.

Chun-Hu, C., Kongara, M. R. and Padture, N.P. (2012), "Site-specific stamping of graphene micro-patterns over large areas using flexible stamps," *Nanotechnology,* vol 23**,** pp. 235603.

De Heer, W.A., Berger, C., Wu, X., First, P. N., Conrad, E. H., Li, X., Li, T., Sprinkle, M., Hass, J., Sadowski, M. L., Potemski, M. and Martinez, G. (2007), "Epitaxial graphene", *Solid State Communications,* vol 143**,** pp. 92-100.

Geim, A. K. and Novoselov, K. S. (2007), "The rise of graphene", *Nature Materials,* vol 6**,** pp. 183-191.

Goler, S., Piazza, V., Roddaro, S., Pellegrini, V., Beltram, F. and Pingue, P. (2011), "Self-assembly and electron-beam-induced direct etching of suspended graphene nanostructures", *Journal of Applied Physics,* vol 110**,** pp. 064308.

Hua, F., Sun, Y., Gaur, A., Meitl, M.A., Bilhaut, L., Rotkina, L., Wang, J., Geil, P., Shim, M., Rogers, J.A. and Shim, A. (2004), "Polymer imprint lithography with molecular-scale resolution", *Nano Letters,* vol 4**,** pp. 2467-2471.

Huang, Y.Y., Zhou, W., Hsia, K.J., Menard, E., Park, J.U., Rogers, J.A. and Alleyne, A.G. (2005), "Stamp collapse in soft lithography", *Langmuir,* vol 21**,** pp. 8058-8068.

Humberto, T., Ruitao, L., Mauricio, T. and Mildred, S.D. (2012), "The role of defects and doping in 2D graphene sheets and 1D nanoribbons", *Reports on Progress in Physics,* vol 75**,** pp. 062501.

Jang, B.Z. and Zhamu, A. (2008), "Processing of nanographene platelets (ngps) and ngp nanocomposites: A review", *Journal of Materials Science,* vol 43**,** pp. 5092-5101.

Janowska, I., Ersen, O., Jacob, T., Vennégues, P., Bégin, D., Ledoux, M.J. and Pham-Huu, C. (2009), "Catalytic unzipping of carbon nanotubes to few-layer graphene sheets under microwaves irradiation", *Applied Catalysis A: General,* vol 371**,** pp. 22-30.

Jayasena, B., Reddy, C.D. and Subbiah, S. (2013), "Separation, folding and shearing of graphene layers during wedge-based mechanical exfoliation", *Nanotechnology,* vol 24**,** pp. 205301-205308.

Jayasena, B. and Subbiah, S. (2011), "A novel mechanical cleavage method for synthesizing few layer graphenes", *Nanoscale Research Letters,* vol 6**,** pp. 95-101.

Jayasena, B., Subbaiah, S. and Reddy, C.D. (2014), "Wedge radius effects in mechanical exfoliation of hopg: a molecular simulation study", *Proceedings of the ASME Manufacturing Science And Engineering Conference*, vol 1, pp. 21-28

Jayasena, R.A.P.B. (2014), *Few layers of graphene and carbon nanoscrolls by wedge based mechanical exfoliation,* Ph.D thesis, Nanyang Technological University.

Kim, S., Wu, J., Carlson, A., Jin, S.H., Kovalsky, A., Glass, P., Liu, Z., Ahmed, N., Elgan, S.L., Chen, W., Ferreira, P. M., Sitti, M., Huang, Y. and Rogers, J.A. (2010), "Microstructured elastomeric surfaces with reversible adhesion and examples of their use in deterministic assembly by transfer printing", *Proceedings of The National Academy of Sciences*, vol. 107, pp. 17095-17100.

Kwanghyun, Y., Yusuke, T., Sungjin, K., Shohei, C., Shigeo, M., Kiyoshi, M. and Isao, S. (2013), "Direct physical exfoliation of few-layer graphene from graphite grown on a nickel foil using polydimethylsiloxane with tunable elasticity and adhesion", *Nanotechnology,* vol 24**,** pp. 205302.

Kymissis, I. and Cox, M. (2013), *Assisted Transfer Of Graphene*, US patent PCT/US2012/071377.

Matthew, A.M., Zheng-Tao, Z., Vipan, K., Keon Jae, L., Xue, F., Yonggang, Y.H., Ilesanmi, A., Ralph, G.N. and John, A.R. (2005), "Transfer printing by kinetic control of adhesion to an elastomeric stamp", *Nature Materials,* vol 5**,** pp. 33-38.

Meihua, J., Hae-Kyung, J., Tae-Hyung, K., Kang Pyo, S., Yan, C., Woo Jong, Y., Eun Ju, R. and Young Hee, L. (2010), "Synthesis and systematic characterization of functionalized graphene sheets generated by thermal exfoliation at low temperature", *Journal of Physics D: Applied Physics,* vol 43**,** pp. 275402.

Meitl, M.A. (2007), *Transfer printing and micro-scale hybrid materials systems*, Ph.D thesis, University Of Illinois at Urbana-Champaign.

Nair, R.R., Blake, P., Grigorenko, A. N., Novoselov, K.S., Booth, T.J., Stauber, T., Peres, N.M.R. and Geim, A.K. (2008), "Fine structure constant defines visual transparency of graphene", *Science,* vol 320**,** pp. 1308.

Novoselov, K.S., Falko, V.I., Colombo, L., Gellert, P.R., Schwab, M.G. and Kim, K. (2012), "A roadmap for graphene", *Nature,* vol 490**,** pp. 192-200.

Novoselov, K.S., Geim, A.K., Morozov, S.V., Jiang, D., Zhang, Y., Dubonos, S.V., Grigorieva, I.V. and Firsov, A.A. (2004), "Electric field effect in atomically thin carbon films", *Science,* vol 306**,** pp. 666-669.

Novoselov, K.S., Jiang, D., Schedin, F., Booth, T.J., Khotkevich, V.V., Morozov, S.V. and Geim, A.K. (2005), "Two-dimensional atomic crystals", *Proceedings of The National Academy of Sciences of The United States Of America,* vol 102**,** pp. 10451-10453.

Ruoff, R. (2008). "Graphene: Calling all chemists", *Nature Nanothnology,* vol 3**,** pp. 10-11.

Song, J., Kam, F.Y., Png, R.Q., Seah, W.L., Zhuo, J.M., Lim, G.K., Ho, P.K.H. and Chua, L.L. (2013), "A general method for transferring graphene onto soft surfaces". *Nature Nanotechnology,* vol 8**,** pp. 356-362.

Stankovich, S., Dikin, D.A., Dommett, G.H.B., Kohlhaas, K.M., Zimney, E.J., Stach, E.A., Piner, R.D., Nguyen, S.T. and Ruoff, R.S. (2006), "Graphene-based composite materials". *Nature,* vol 442**,** pp. 282-286.

Sun, G., Li,X., Qu, Y., Wang, X., Yan, H. and Zhang, Y. (2008), "Preparation and characterization of graphite nanosheets from detonation technique", *Materials Letters,* 62**,** 703-706.

Whitesides, G.M., Ostuni, E., Takayama, S., Jiang, X. and Ingber, D.E. (2001), "Soft lithography in biology and biochemistry", *Annual Review Of Biomedical Engineering,* vol 3**,** pp. 335-373.

Wu, Z.S., Ren, W., Gao, L., Zhao, J., Chen, Z., Liu, B., Tang, D., Yu, B., Jiang, C. and Cheng, H.-M. (2009), "Synthesis of graphene sheets with high electrical conductivity and good thermal stability by hydrogen arc discharge exfoliation", *ACS Nano,* vol 3**,** pp. 411-417.

Xia, Y. and Whitesides, G.M. (1998), "Soft lithography", *Angewandte Chemie International Edition,* vol 37**,** pp. 550-575.

Xuekun, L., Minfeng, Y., Hui, H. and Rodney, S.R. (1999), "Tailoring graphite with the goal of achieving single sheets", *Nanotechnology,* vol 10**,** pp. 269.

Zang, J., Ryu, S., Pugno, N., Wang, Q., Tu, Q., Buehler, M.J. and Zhao, X. (2013), "Multifunctionality and control of the crumpling and unfolding of large-area graphene", *Nature Materials,* vol 12**,** pp. 321-325.

Zhang, Y.B., Small, J. P., Pontius, W.V. and Kim, P. (2005), "Fabrication and electric-field-dependent transport measurements of mesoscopic graphite devices", *Applied Physics Letters,* vol 86**,** pp. 073104-073107.